1 # Predicting resprouting of *Platanus × hispanica* following branch

2 # pruning by means of machine learning

3

4 Qiguan Shu[1](0000-0003-3856-2191), Hadi Yazdi[1](0000-0002-1429-5642), Thomas

5 Rötzer[2](0000-0003-3780-7206), Ferdinand Ludwig[1](0000-0001-5877-5675)

6 1 Professorship for Green Technologies in Landscape Architecture, TUM School of

7 Engineering and Design, Technical University of Munich, Germany

8 2 Chair for Forest Growth and Yield Science, Technical University of Munich, Germany

9 For correspondence: qiguan.shu@tum.de, +49 89 289 28041

10

11 ## Summary

12 - Resprouting is a crucial survival strategy following the loss of branches, being it by

13 natural events or artificially by pruning. The prediction of resprouting patterns on a

14 physiological basis is a highly complex approach. However, trained gardeners try to

15 predict a tree's resprouting after pruning purely based on their empirical knowledge

16 and a visual check of the tree's geometry. In this study, we explore in how far such

17 predictions can also be made by algorithms, especially using machine learning.

18 - Table-topped annually pruned *Platanus × hispanica* trees at a nursery were

19 documented with terrestrial LiDAR scanners in two consecutive years. Topological

20 structures for these trees were abstracted from point clouds by cylinder fitting. Then,

21 new shoots and trimmed branches were labelled on corresponding cylinders. Binary

22 and multiclass classification models were tested for predicting the location and

23 number of new sprouts.

24 - The accuracy for predicting whether having or not new shoots on each cylinder

25 reaches 90.8% with the LGBMClassifier, the balanced accuracy is 80.3%. The

26 accuracy for predicting the exact numbers of new shoots with GaussianNB model is

27 82.1% but its balanced accuracy is reduced to 42.9%.

28 - The results were validated with a separate evaluation dataset. It proves a feasibility in

29 predicting resprouting patterns after pruning using this approach. Different tree species,

30 tree forms, and other variables should be addressed in further research.

31

Keywords

33 tree manipulation, branch pruning, resprout pattern, TLS, tree QSM, machine learning

34

Word counts

36 Introduction 1272 words;

37 Materials and Methods 2463 words;

38 Results 488 words;

39 Discussion 579 words;

40 Conclusion 452 words;

41 5 Figures;

42 4 Tables;

43

1.   Introduction

45 Disturbances to tree growth like ice storms, fires, wind and diseases (Hauer et al., 2006;

46 Simler et al., 2018) are common in nature. They cause great loss in trees' biomass especially

47 above the ground. In view of this, resprouting is a vital survival strategy for most tree species:

48 new shoots can grow out of dormant buds rapidly at certain positions after the disturbance

49 occurred. This process is recognized as a major force in forest regeneration (Matula et al.,

50 2019) and has significant impacts on forest dynamics (Martini et al., 2008). Humans

51 recognized and harnessed these phenomena from early times (Candel-Pérez et al., 2022; Petit

52 & Watkins, 2003). A famous example is pollarding, where all the shoots of a tree crown are

53 regularly cut off to encourage the growth of new sprouts, which were used as firewood and

54 material for weaving baskets.

55 Regardless of the practical use, it is a highly interesting but at the same time very complex

56 challenge to understand and predict the resprouting patterns of trees caused by disturbances

57 on a physiological basis. These patterns are firstly determined by axillary buds which either

58 form new shoots or enter dormancy (Suzuki, 2002). This "decision" is essentially controlled

59   by hormone signals. Auxin was considered one of the main mediator in the 20th century,

60   while new findings indicate that cytokinins (Salam et al., 2021; Schneider et al., 2022) and

61   strigolactones (Gomez-Roldan et al., 2008) play a major role in apical dominance and

62   branching inhabitation respectively. Without a clear conclusion yet regarding their exact

63   mechanisms, studies tried to understand resprouting patterns from other micro and macro

64   perspectives: its relation to genetic regulation (Hill & Hollender, 2019), in responding to

65   seasonal adaptation (Singh et al., 2022), or by an explanation known as Low Energy

66   Syndrome (Martín-Fontecha et al., 2018).

67   However, these endogenous physiological processes do not tell the whole story of resprouting.

68   Leaf area and light are redistributed after the disturbances, which then affects photosynthetic

69   processes (Balandier et al., 2000). This does not simply mean a decrease in photosynthetic

70   capacities, but involves reallocation of carbon- and other resources among plant organs such

71   as fruits (Kohek et al., 2015; Tosto et al., 2023) and flowers (Grechi et al., 2022). What makes

72   the impact of this disturbance even more complex is timing. For example, summer pruning on

73   an apple tree normally causes a temporary loss of apical dominance and increase its cytokinin

74   supply. But depending on its exact timing, the dominance may be delayed or even prevented

75   (Saure, 1987). As a result, a precise analysis of how a disturbance reshapes a tree using a

76   physiological approach must address 1) primary status of hormone, 2) resource reallocation,

77   and 3) timing issue. To our knowledge no research has brought all these aspects together so

78   far.

79   Even without any precise analytical tools regarding resprouting analysis, skilled practitioners

80   learn how to prune a tree in their charge. They neither measure its sap-flows with multiple

81   sensors nor meter the cytokinin concentration in chemistry labs. By going around the tree and

82   observing the main branches, they decide where to prune. Their decisions are based on

83   empirical knowledge of natural phenomena, originally derived from accurate observations of

84   causes and effects – the tree's resprouting reaction to the loss of branches by pruning.

85   Countless repetitions of similar processes have been experimented in horticulture over

86   centuries (Saunders, 1898). For a gardener, his or her primary pruning skills may start with a

87   set of general rules written in a manual book (Brickell & Joyce, 1996). Then, their skills will

88   independently evolve further through repeated practices at work specific to different climate

89   zones, species etc. If their pruning decisions lead to resprouting reactions largely similar to

90   their expectations, gardeners finally prove to be able to predict the tree's reaction purely on

91   visual observation and geometrical patterns without digging deep into simulating

92   physiological processes.

93   In horticulture and arboriculture, we currently see a strong trend towards automation of

94   pruning by machines or robots (Sam et al., 2022). So far, these are comparatively simple,

95   standardized actions (M. Li et al., 2021; Sam et al., 2022), but the more complex the tasks

96   become in this regard, the more important is a plausible, robust and prompt prediction of the

97   growth reaction of a tree to pruning. At the same time, it can be assumed that in the future

98   trees worldwide will increasingly experience growth disturbances due to the consequences of

99   climate change (drought, stronger and more frequent storms), which will be coupled with a

100   loss of biomass and subsequent resprouting. In order to assess the development of such trees,

101   for example in an urban context, also here a plausible, robust and prompt prediction of

102   resprouting in response to the previous loss of branches and twigs is necessary.

103   In this regard, physiological forecasts are too complex, rely on too many often-unknown

104   parameters (e.g. weather) and thus are too sensitive to errors and too slow. The aim of the

105   study at hand is to develop first basics for a prediction model on the basis of geometric

106   patterns corresponding to the approach of experienced gardeners using a concrete example.

107   Rapid development in remote sensing is providing a solid base for this aim. First of all,

108   terrestrial LiDAR scanners can capture detailed geometry of objects with a precision up to 3

109   mm from multiple standing positions (RIEGL, 2023). This method proves capable of

110   capturing a tree's trunk and branches with more than 10 mm diameter (Gobeawan et al., 2018;

111   Yang et al., 2022) during its leaf-off state (Kükenbrink et al., 2022). Raw data is stored in the

112   form of a discrete point cloud. Furthermore, different approaches have been developed to

113   extract tree structure: skeleton abstraction following occupancy grids (Bucksch et al., 2010;

114   Sun et al., 2022); branch direction by eigenvectors of point patches or sections (Bremer et al.,

115   2013; Raumonen et al., 2013); skeleton as the Dijkstra's shortest path from the tree base to

116   ends (Du et al., 2019; J. Li et al., 2022, 2022; Wang et al., 2014); skeleton redrawn with

117   searching steps (Hackenberg et al., 2014); learning the reconstruction pattern through a neural

118   network (Liu et al., 2021). Overall, these abstracted information about tree architecture is

119   called quantitative structure model (QSM) (Åkerblom et al., 2017; Shu et al., 2022). In this

120   way, every segment of the tree stem or branch can be retrieved containing its diameter, length,

121   axial direction, hierarchy in the whole branching structure as well as the pointer to its parent

122   and child segments.

123   These data for a computational model are like experiences for a human brain. The process for

124   an algorithm to "learn from experience" without being explicitly programmed was defined as

125   machine learning (Samuel, 1959). Over 70 years of development, machine learning models

126   have proven capable and efficient to inherently solve the 5 typical problems of data science,

127   namely classification, anomaly detection, regression, clustering and reinforcement learning

128   (Alzubi et al., 2018). Among them, classification models can assign class labels to testing

129   instances where the predictor features are known (Kotsiantis, 2007). Depending on the

130   number of output labels, they work for both binary and multi-class classification problems. To

131   establish such models from a practical aspect, open-source packages such as scikit-learn

132   (Pedregosa et al., 2011) have integrated common ones, offering an easy access to adapt

133   parameters for different applications.

134   Equipped with the digital tools above, accurate information regarding tree structures can be

135   collected and processed in analogy to what a real gardener does. Building on this, we are

136   addressing the following questions: How can we predict the position and number of

137   resprouting shoots based on a purely "visual approach" (pattern recognition)? Which machine

138   learning model achieves the best accuracy for this task?

139

140   ## 2.   Materials and Methods

141   ### 2.1 Study case

142   To address our questions, we looked for tree cases that are frequently pruned in a distinct

143   manner under similar environmental conditions. At Bruns Nursery, Bad Zwischenahn in the

144   north of Germany, so-called table-topped plane trees (*Platanus × hispanica*) are grown in a

145   clearly defined area under standardized conditions. The crowns of these tree are shaped into a

146   flat layer through labour-intensive maintenance. This form probably origins from Baroque

147   gardens, where plants were kept in an orthogonal manner to enhance the orientation or

148   perspective (Dobrilovič, 2010). Due to the expansion of the crown like an umbrella, it is still

149   used in European cities nowadays for shading squares and pedestrian areas (e.g., the central

150   square at Labouheyre, France). To produce such trees, there are in general two phases. In the

151   first phase, a young plane tree with a naturally grown canopy is intensively trimmed. At

152   around 3 meters height six branches are selected and bent horizontally into different directions

153   with equal angles in between. Where necessary, bamboo sticks are added as temporary

154   supports to force the branch into the aimed direction (see "1st year" in Fig. 1). In the second

155   phase, new shoots or even some of the older shoots from these six main branches are carefully

156   selected and pruned by experienced gardeners. Pruning decisions are important at this phase

157   to enable shoot growth only at desired positions. Some shoots reserved from previous years

158 could still be trimmed off if there appears another new shoot that becomes a better option.

159 This procedure is repeated in the following years (see "2nd-6th year" in Fig. 1). Multiple

160 reiterations of the tree by resprouting result in a complex branching pattern. Due to the annual

161 pruning and relative complex branching pattern the second phase of these cases is considered

162 effective to analyse abilities of machine learning models in predicting resprouting patterns

163 based on quantitative structural tree models under complex yet repetitive conditions. It should

164 be noticed that the aim of this study is not recreating this specific form of tree geometry like

165 the table-topped *Platanus × hispanica* but to gain fundamental knowledge regarding

166 resprouting reactions of trees.
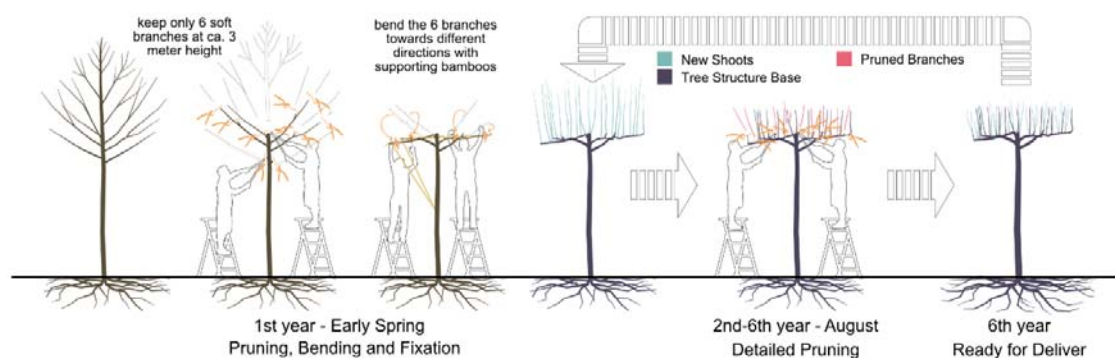

167

168 Figure 1. The procedure for producing a table-topped *platanus* through iterative branch and

169 shoot selection and pruning with intensive labour force.

170 2.2 Data acquisition and pre-processing

171 In subsequent two winters, namely in January 2022 and January 2023, an area consisting of 3-

172 and 4-year-old table topped platanus (see Fig. 2a) planted in 3 rows at Bruns Nursery were

173 scanned with LiDAR scanner RIEGL VZ-400i. The scanner was mounted on a tripod in 2022,

174 while mounted on a vehicle (see Fig. 2b) in 2023. All the scans were set to "Panorama30"

175 standard (with angular resolution 0.030°) and conducted in a "stop-and-go" method. Scanning

176 positions were located along each row at every third tree (ca. 12 m). Point clouds from

177 different scan positions were automatically registered in RiSCAN Pro in reference to GNSS

178 coordinates recorded with Leica Zeno FLX100 plus (Leica, 2023). The original GNSS

179 coordinates indicate accuracies ranging between 0.68 to 0.80 m at different scan positions.

180 Therefore, the reliability on GNSS was set to low during the automatic registration and the

181 multistation adjustment. With all steps above, we got two point clouds containing all the tree

182 cases for the year 2022 and 2023 respectively. Afterwards, individual trees were segmented

183 manually (see Fig. 2c). This manual step is efficient for our cases because those trees planted

184   in the nursery were almost perfectly aligned in an equal distance and their crowns did not

185   touch each other. The ground surface was flat and clear and there were no irrelevant objects

186   such as shrubs around tree trunks. A total of 49 plane trees were scanned in 2022 while the

187   number of trees scanned in 2023 was 28, (due to tree sales during 2022, see Fig. 2d and 2e).

188   As a result, we got point clouds of 28 plane trees for both years.

189   The next step was to identify changes in the geometrical structure of the trees in these two

190   years (see Fig. 2h). For this purpose, the two corresponding scans regarding the same trees

191   must be aligned. The GNSS coordinates have an offset up to 0.8 meters, which is not

192   sufficient to our demand. The most common algorithm for matching 3d models precisely,

193   namely Iterative Closest Point (Rusinkiewicz & Levoy, 2001), does not work for these tree

194   cases because the new shoots and the extensive pruning on tree branches have altered their

195   geometries significantly. A supervised alignment by manually picking point pairs on

196   corresponding branch surfaces also caused visible deviations owing to the girth growth.

197   Finally, we manually aligned all tree pairs individually using multiple views. This guaranteed

198   the best possible alignment despite significant geometrical changes between the two scans.

199   Only then, we were able to precisely detect the changes caused by growth and pruning

200   between the point clouds. In principle, point sets that only appeared in the scan of 2022 and

201   disappeared in the scan of 2023 should represent branches pruned away. Conversely, point

202   sets that were only found in 2023 should represent new shoots. In practice, however, an object

203   even with no change in its geometry is unlikely to have identical points on its surface in the

204   two independent scans. To solve this, cloud-to-cloud distance (Jafari et al., 2017) was applied.

205   It calculates the distance between each point in one point cloud to its nearest neighbour in the

206   other point cloud using Hausdorff distance algorithm (Girardeau-Montaut, 2023). Depending

207   on point cloud quality and precision in alignment, a minimum distance threshold ranging

208   between 0.020 to 0.045 m was customized to each point cloud for segmenting unchanged and

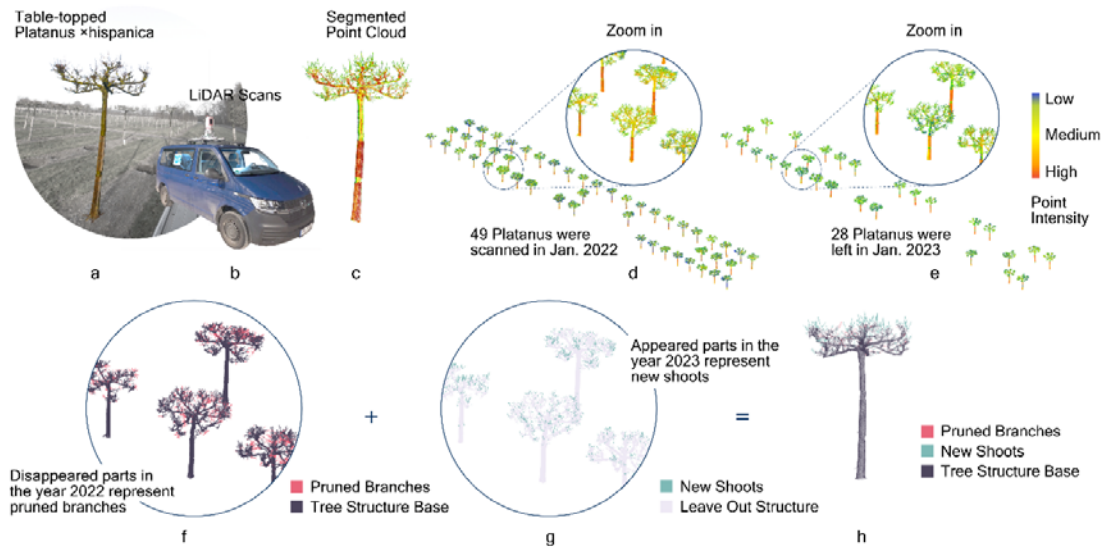209   changed parts (see Fig. 2f and 2g).

210

211   Figure 2. The overall procedure for detecting pruned branches and new shoots from point

212   clouds of LiDAR scans of two consecutive years.

213   Parallel to change detection, the point clouds were also used to create quantitative structural

214   models (QSMs) of the trees (see Fig. 3a) by TreeQSM (Raumonen et al., 2013) in MATLAB

215   (The MathWorks Inc., 2023) (see Fig. 3b). Some other QSM reconstructing programs like

216   AdTree (Du et al., 2019) and AdQSM (Fan et al., 2020) build tree structures by the Dijkstra's

217   shortest path and the minimum spanning tree. They appeared to be sensitive to outliers in our

218   dataset. Especially when they built detailed twigs at the branch's high end, many shoots were

219   invented by the algorithm due to outliers, not reflecting the actual sprouting pattern. In

220   comparison to them, TreeQSM fits cylinders to point patches in defined sizes. This approach

221   performs better in noise and outlier resistance than those methods using the Dijkstra's shortest

222   path. For each point cloud, we tested 18 configurations of different settings regarding the

223   patch sizes for reconstructing the QSMs in TreeQSM. For each configuration, the

224   reconstruction was repeated 15 times to reduce the impacts of pseudo-random numbers in this

225   TreeQSM process. Finally, the QSM with minimum mean distances from points to trunk and

226   branch cylinders was chosen as the model for the corresponding point cloud. It should be

227   addressed again that each tree is represented with two point clouds, and accordingly two

228   QSMs, showing their situations in 2022 and 2023 respectively. To further ensure a precise

229   reconstruction, the outliers were pre-deleted through the statistical outlier removal tool (Rusu

230   & Cousins, 2011).

231   2.3 Labelling and reorganizing the dataset

232 In the pre-processing, the trimmed branches as well as the new shoots were detected in the

233 point clouds while topological cylinders were generated with TreeQSM. The next step was to

234 combine these two datasets. The individual cylinders of the QSMs must be labelled as to

235 whether they are part of an unchanged branch (not considering the girth growth), a pruned

236 branch or a new shoot. This was achieved by making use of a distance threshold between

237 points of the cylindrical axis and their nearest neighbouring point of the segmented point

238 clouds. For our data, we examined only the start and the end point of every cylinder. If the

239 sum of their mean distances to their 10 nearest neighbours with the same label (i.e., trimmed

240 branches) was below 100 mm, this cylinder was also labelled the same (see Fig. 3c 3f). To

241 enhance the accuracy of the labelling, three more criteria were added based on practical rules

242 when pruning these trees: for any cylinder labelled as part of either a new shoot or a pruned

243 branch, its radius must be smaller than 20 mm (one year old shoots do not reach more than 20

244 mm in diameter for the trees at hand); for any cylinder labelled as part of a pruned branch, its

245 branch hierarchical order must be larger than 1 (not the tree trunk and the primary branch);

246 the label for trimmed branches and new shoots on one cylinder is passed on to all its children

247 cylinders.

248 After labelling, the cylinders of different labels (unchanged branches, pruned branches and

249 new shoots) are still separated in two QSMs regarding the same tree. There are no

250 correspondences between these two QSMs as their reconstruction processes are independent.

251 Therefore, cylinders of the trimmed branches in one QSM must be integrated into the other

252 QSM that contains the main tree structure and the new shoots, or reversely, cylinders of new

253 shoots must be integrated into the QSM with the trimmed branches. This is a tricky process.

254 While the geometric data remain the same for every cylinder, its topological data regarding

255 the ID of the cylinder, its parent cylinder and its child cylinder must be corrected, as well as

256 the branch order and its position in the branch. Regarding whether to transfer cylinders of new

257 shoots or pruned branches to the other QSM, considerations can be described as follows. The

258 pruned branches, in general, could only be the same size or thicker than the new shoots.

259 Consequently, cylinders of pruned branches have higher robustness in their position through

260 cylinder fitting. As a result, the certainty for redefining their topological parent in another

261 QSM based on their relative positions is supposed to be higher. So, for our dataset, the

262 cylinders of pruned branches were picked out from their original QSM and integrated into the

263 other QSM that has the new shoot cylinders (see Fig. 3e). Their new parent cylinders were

264 redefined as those whose end points were located closest to their starting point. Based on this,

265   the topological data for every single cylinder in the newly merged QSM were completely

266   overwritten due to this change.

267   Finally, the total number of pruned branches and new shoots on every cylinder was counted

268   (see Fig. 3d). This became the crucial attribute for the prediction models in the next step.
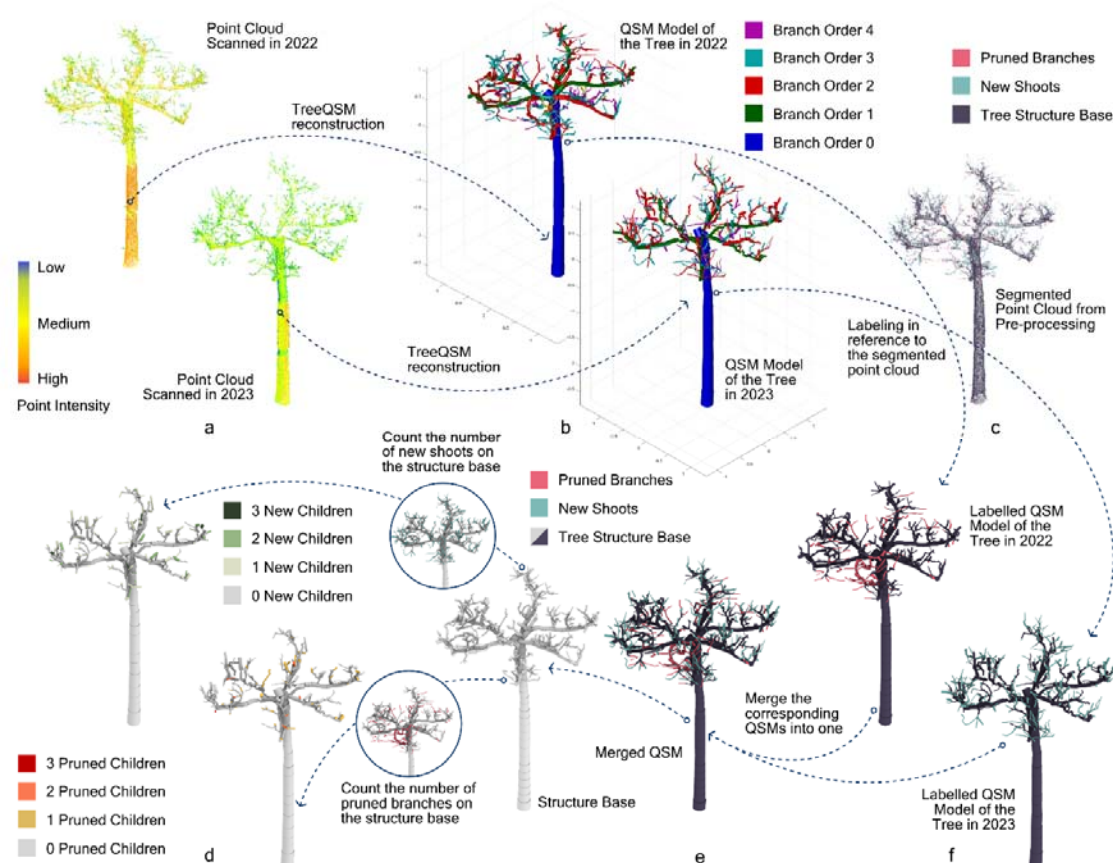
269

270   Figure 3. Overall procedure for labelling and reorganizing the dataset.

271   2.4 Prediction with various classification models

272   The dataset after all the processes described above contains 34,245 items, representing 28

273   table topped plane trees. Each item corresponds to one cylinder, which contains the following

274   attributes: tree's ID; cylinder's ID; parent cylinder's ID; child cylinder's ID in the same

275   branch; x-y-z coordinate of the cylinder start; a normalized 3d vector of the axial direction;

276   branch's ID; its sequence in the branch; branch order; cylinder length; cylinder radius; the

277   number of pruned children and new children; the Boolean value if this cylinder is virtually

278   added during QSM reconstruction; the Boolean value if this cylinder is pruned out.

279   The relationships between each two attributes (except for the IDs and Boolean values) are

280   illustrated in appendix 2. For our research purpose, the sprout location and numbers are the

281   label of new shoots on each cylinder. We tested classification models in machine learning for

282   finding links between these topological and geometrical attributes and the predicting target.

283   Among these target labels, 16,183 (47.3%) cylinders were labelled "-1" meaning that they are

284   trimmed away. These cylinders are not feeding into machine learning models. 15,348 (44.8%)

285   cylinders have no new shoot, thus labelled with "0". 2,329 (6.8%) cylinders have one new

286   shoot (labelled "1"). There are less cylinder samples, whose new shoot number is larger than

287   "1": 321 (0.94%) cylinders have 2 new shoots; 54 (0.16%) cylinders have 3 new shoots; 7

288   (0.02%) cylinders have 4 new shoots; 2 cylinders have 5 new shoots; only 1 cylinder has 6

289   new shoots on it. Due to the extreme rare samples with a high number of new shoots, we label

290   those cylinders that have more than 4 shoots with new shoot number 4.

291   Owing to the limited volume of data we acquired, the majority of the items labelled with new

292   shoot number from "0" to "4" must feed into machine learning models (16,558 items

293   representing 26 trees). Nevertheless, we reserved 2 trees (1,504 items) as an evaluation

294   dataset. This evaluation dataset was only used for validating the results (see section 3), not for

295   training the model. The dataset for machine learning was further divided into a training set

296   (13,246 items) and a testing set (3,312 items, with a test size of 0.2). The testing set prevented

297   overfitting the models to the given data.

298   For getting a quick overview of the performances across a wide range of classification models

299   in machine learning on the dataset, we used lazy predict (Pandala, 2023) to run scikit-learn

300   (Pedregosa et al., 2011) to compare 25 common classification models with their default

301   settings, including GaussianNB, NearestCentroid and LGBMClassifier. Besides, we tested a

302   basic Artificial Neural Network model (ANN) built with Keras (Chollet, 2015). It consisted of

303   two hidden layers with 64 and 128 nodes respectively (see Fig. 4 left). In addition, to examine

304   a graph neural network (GNN) model, the dataset for each tree was processed to a graph

305   (Salama, 2021), where every cylinder item was a node connected to its parent and children

306   (the node connection for one tree is illustrated in Fig. 4 right). These graph data were fed into

307   a GNN model named "baseline classifier" (see table 2.1) including 39,512 trainable params

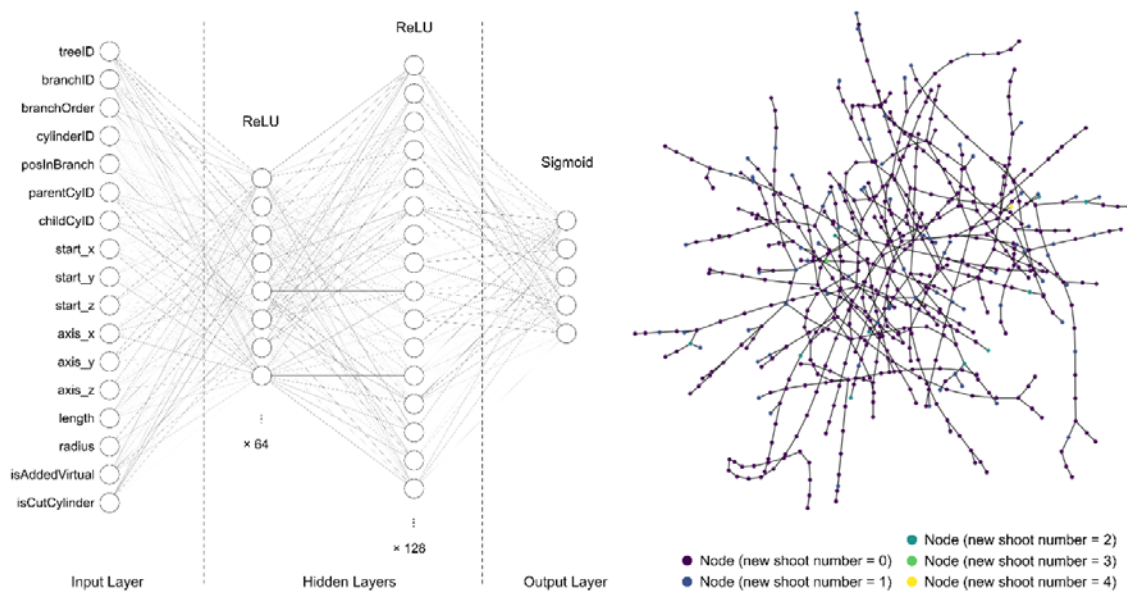308   and 1,174 non-trainable params.

309

310   Figure 4. Architecture of the ANN (left) and Graph (right) of one tree used in our test.

311   Table 2.1. Architecture of the GNN model in our test.

Layer (type)	Output Shape	Param	Connected to
input_features (InputLayer)	[(None, 11)]	0	[]
ffn_block1 (Sequential)	(None, 64)	5228	['input_features[0][0]']
ffn_block2 (Sequential)	(None, 64)	8832	['ffn_block1[0][0]']
skip_connection2 (Add)	(None, 64)	0	['ffn_block1[0][0]', 'ffn_block2[0][0]']
ffn_block3 (Sequential)	(None, 64)	8832	['skip_connection2[0][0]']
skip_connection3 (Add)	(None, 64)	0	['skip_connection2[0][0]', 'ffn_block3[0][0]']
ffn_block4 (Sequential)	(None, 64)	8832	['skip_connection3[0][0]']
skip_connection4 (Add)	(None, 64)	0	['skip_connection3[0][0]', 'ffn_block4[0][0]']
ffn_block5 (Sequential)	(None, 64)	8832	['skip_connection4[0][0]']
skip_connection5 (Add)	(None, 64)	0	['skip_connection4[0][0]', 'ffn_block5[0][0]']
logits (Dense)	(None, 2)	130	['skip_connection5[0][0]']

312

313   We tested all these classification models in two manners of labelling: binary labels that only

314   classify cylinders if they will or will not grow new shoots, and multiclass labels that classify

315   cylinders based on the exact number of new shoots ranging between 0 to 4.

316

317   3.   Results

318   The accuracy, balanced accuracy, and F1 Score (weighted average F1 score for multiclass

319   labels) of the tested models in a default setting or with a basic architecture (see section 2.4)

320   are listed in Fig. 5. Each scoring index ranges between 0 and 1. 1 is the best score, meaning

321   that all the shoot labels are correctly predicted. On the contrary, 0 is the worst score,

322   representing no correct prediction. In the figure, these models are shown in a descending

323   order from the left to the right according to their total scores in classifying binary labels.

324   Among the three sub-scores, accuracy reflects an overall rate of true predictions for all labels.

325   Our datasets are imbalanced in terms of different label numbers. Therefore, balanced accuracy,

326   which gives equal weights to the true prediction rates for each label, is also an important

327   indicator in evaluating their performances. F1 score is another effective index for the

328   imbalanced classifications but attaches more importance to true positives (predicting the

329   cylinders with new shoots correctly) while it ignores the true negatives (predicting the

330   cylinders with zero shoot correctly). Based on these benchmark scores, LGBMClassifier and

331   GaussianNB have top scores for predictions with binary and multiclass labels respectively.

332   The confusion matrix of the LGBMClassifier with binary labels in testing set is shown in

333   table 3.1. The confusion matrix of the GaussianNB model with multiclass labels in testing set

334   is shown in table 3.2.
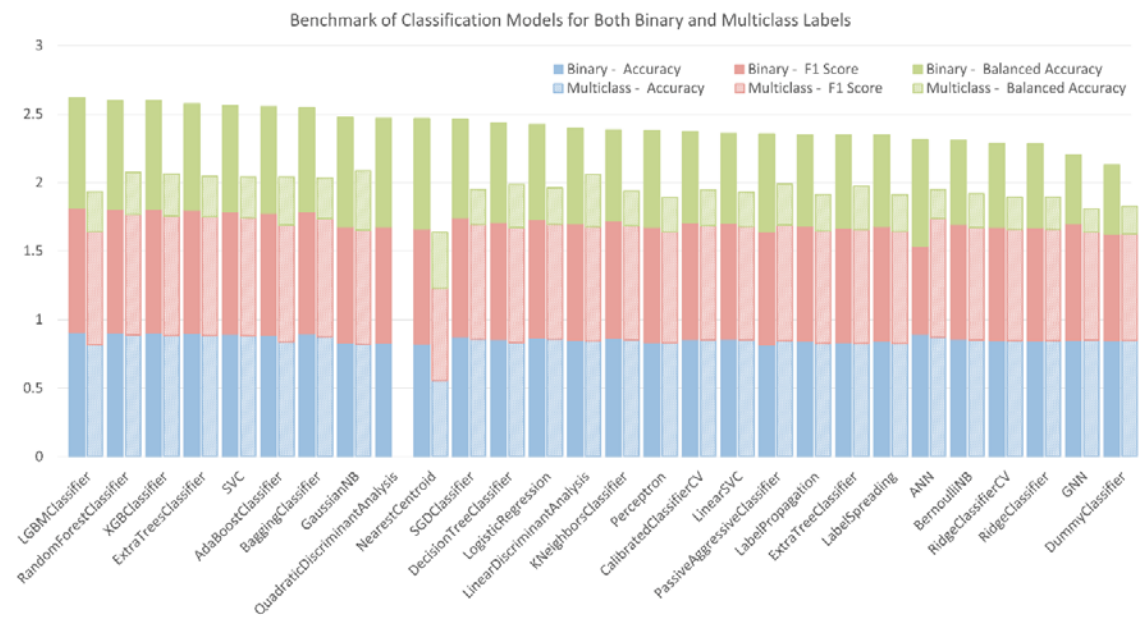

335

336   Figure 5. Benchmark of tested classification models for binary and multiclass labelling.

337   Table 3.1. Confusion Matrix of LGBMClassifier with Binary Labels in Testing Set

	Negative / 0	Positive / 1
Negative / 0	2883 (79.8%)	170 (4.7%)
Positive / 1	209 (5.8%)	351 (9.7%)

338

339   Table 3.2. Confusion Matrix of GaussianNB Model with Multiclass Labels in Testing Set

	0	1	2	3	4
0	2458 (74.2%)	309 (9.3%)	33 (1.0%)	0 (0%)	1 (0%)
1	153 (4.6%)	258 (7.8%)	24 (0.7%)	0 (0%)	3 (0.1%)
2	29 (0.9%)	27 (0.8%)	5 (0.2%)	0 (0%)	0 (0%)
3	4 (0.1%)	4 (0.1%)	0 (0%)	0 (0%)	1 (0%)
4	2 (0.1%)	1 (0%)	0 (0%)	0 (0%)	0 (0%)

340

341   To further validate these two models, we applied the trained LGBMClassifier model and

342   GaussianNB model to the evaluation set with binary and multiclass labels respectively. The

343   results of the evaluation are visually illustrated in supplementary material. Their accuracy,

344   balanced accuracy and F1 Score on the validation set in comparison to the testing set is shown

345   in table 3.3. The accuracy, balanced accuracy and weighted F1 score at the evaluation set

346   (only 2 trees) have maximum around 10% difference to the scores on the benchmark.

347   Table 3.3. Scores of LGBMClassifier and GaussianNB Model in Evaluation Set

	Scores in testing set			Scores in evaluation set		
	Accuracy	Balanced accuracy	F1 Score	Accuracy	Balanced accuracy	F1 Score
LGBMClassifier with binary labels	0.91	0.80	0.91	0.91	0.81	0.91
GaussianNB Model with multiclass labels	0.82	0.43	0.84	0.93	0.30	0.83

348

349   4.   Discussion

350   In order to be able to meaningfully interpret and evaluate the results, it is first necessary to

351   discuss the specific conditions of the dataset and resulting limitations.

352   The following factors may impact on the accuracy of the extracted geometrical data from the

353   trees: 1) To prevent browsing the tree barks, protecting covers were installed at a height below

354   2 meters around the tree trunks. This might have caused the diameter measured at trunk

355   cylinders to be slightly overestimated. However, we assume that this has no influence on the

356   prediction model. 2) Minor swinging of the branches by wind during the LiDAR scanning

357   might have caused outliers or might have led to overestimating the diameter of the smaller

358   branches. Although the point clouds were denoised through SOR filters, this does not

359   guarantee full deletion of these outliers and could then cause inexistent branches in the

360   cylindrical models. 3) Aligning the same trees with different geometries in the two years is a

361   nonstandard manual process so far, which can cause inconsistence in change detection and

362   identification of parent cylinders. A possible alternative to detect these changes is comparing

363   the occupancy grids (Hirt et al., 2021).

364   The total cylinder numbers for training the models were limited to 16,558 items representing

365   26 trees. The percentage of the negative label "0" makes up more than 92% of the total items,

366   causing an unbalanced rate for the number of positive samples (less than 2500 items).

367   Unfortunately, these are all available data from the nursery.

368   Most importantly, the collected dataset in two consecutive years reflects the growth of these

369   trees under almost identical environmental conditions and pruning regime. More specifically,

370   the temperature, water content in the soil, wind direction and speed as well as the time of

371   pruning are all the same for these trees. This means that our method can predict the

372   resprouting pattern of this kind of table-topped plane trees grown under the same conditions

373   as in this study at current stage. In case of any changes in the factors mentioned above, it is

374   unclear so far how accurate the prediction will be. For instance, the model may not predict

375   the growth of the same trees in the following year, because horticultural experience shows

376   that a change in the time of pruning of only one or two weeks can have a significant impact on

377   the growth of new shoots, especially if there is also a change in weather conditions (e.g. heat

378   or drought immediately after pruning).

379   For understanding whether those environmental factors could also be addressed in a

380   prediction model in the same approach, these environmental data must be collected and

381   coupled with a larger quantity of trees. This hints to an upcoming step of this study.

382   Finally, the current model is only the first step in understanding resprouting patterns after one

383   specific artificial disturbance, namely pruning of table topped trees. Nonetheless we are

384   optimistic that the approach has great potential for further development and application (see

385   e.g., (Yazdi et al., 2023)). The application of such model is not limited to repeat what the

386   gardeners can already do but go beyond knowledge boundaries regarding the resprouting

387   strategy of trees after disturbances. This can hopefully be achieved through gathering a huge

388   amount of data. By searching through this database, the "digital gardener" is likely to find

389   evidence to support its predictions in a more complex context. For this far vision, an open-

390   source and uniformed database about trees (Shu et al., 2022) is required.

391

5.   Conclusion

393 Resprouting patterns are key in understanding regeneration of trees after natural and artificial

394 disturbances. The interrelationships are very complex, involving among other things the

395 primary status of hormones, the redistribution of resources, and timing issues. Until now, no

396 single model can address all these factors in a physiological approach. However, gardeners

397 and practitioners have been trained to prune trees based on their intuitive predictions since

398 centuries. They are able to do so based on accumulated knowledge working with trees. In this

399 study, we gave it a first try addressing the question if computational models, especially

400 machine learning models could gain similar knowledge as practitioners from horticulture:

401 what are the location and numbers of new shoots after pruning? Which model would achieve

402 the best performance?

403 For this purpose, we scanned a group of annually pruned plane trees at a tree nursery with

404 LiDAR. The detailed geometry and topology of the branches were extracted through

405 quantitative tree models. The trimmed branches and new shoots were detected through

406 comparison between the scans in two consecutive years and this information were finally

407 labelled on a dataset for training multiple classification models.

408 We tested 25 common classification models in the field of machine learning with default

409 settings. Additionally, 1 ANN model and 1 GNN model with most basic architectures were

410 also tested. Among these models, except for two, all other models have an accuracy and a F1

411 score higher than 80%. For balanced accuracy, the average score of all the models was ca. 70%

412 for binary labels; for multiclass labels, the average was 28.3%.

413 From the results, we can conclude that for the collected dataset, most of the models work well

414 in telling the position of new shoots but are not accurate in telling the actual shoot numbers at

415 the specific location. For the best scored models with binary labelling, the LGBMClassifier

416 can predict the position of new shoots with an accuracy of 90.8% and a balanced accuracy of

417 80.3%. For predicting the exact number of the shoots, GaussianNB Model performs the best.

418 The accuracy is 82.1% because most of the cylinders should have the shoot number 0.

419 However, the balanced accuracy is reduced to 42.9%.

420 The limitation of the current model is definitely very specific to the studied site,

421 environmental conditions, tree species and form, and the pruning time. In the next step, a

422 larger amount of tree data is being collected in the city of Munich to analyse how this

423   approach can be extended to a larger scope addressing maybe some of the environmental

424   factors. In a further vision, a huge database of the "digital gardener" would push forward the

425   knowledge boundaries in understanding resprouting strategies of trees facing natural and

426   artificial disturbances.

427

Acknowledgement

437

References

439   Åkerblom, M., Raumonen, P., Mäkipää, R., & Kaasalainen, M. (2017). Automatic tree species

440   recognition with quantitative structure models. *Remote Sensing of Environment*, *191*,

441   1–12. https://doi.org/10.1016/j.rse.2016.12.002

442   Alzubi, J., Nayyar, A., & Kumar, A. (2018). Machine Learning from Theory to Algorithms:

443   An Overview. *Journal of Physics: Conference Series*, *1142*(1), 012012.

444   https://doi.org/10.1088/1742-6596/1142/1/012012

445   Balandier, P., Lacointe, A., Roux, X. L., Sinoquet, H., Cruiziat, P., & Dizès, S. L. (2000).

446   SIMWAL: A structural-functional model simulating single walnut tree growth in

447   response to climate and pruning. *Annals of Forest Science*, *57*(5), 571–585.

448   https://doi.org/10.1051/forest:2000143

449   Bremer, M., Rutzinger, M., & Wichmann, V. (2013). Derivation of tree skeletons and error

450   assessment using LiDAR point cloud data of varying quality. *ISPRS Journal of*

451 *Photogrammetry and Remote Sensing*, *80*, 39–50.

452 https://doi.org/10.1016/j.isprsjprs.2013.03.003

453 Brickell, C., & Joyce, D. (1996). Royal Horticultural Society: Pruning & training. *Royal*

454 *Horticultural Society: Pruning & Training.*

455 https://www.cabdirect.org/cabdirect/abstract/19970300717

456 Bucksch, A., Lindenbergh, R., & Menenti, M. (2010). SkelTre. *The Visual Computer*, *26*(10),

457 1283–1300. https://doi.org/10.1007/s00371-010-0520-4

458 Candel-Pérez, D., Hernández-Alonso, H., Castro, F., Sangüesa-Barreda, G., Mutke, S.,

459 García-Hidalgo, M., Rozas, V., & Olano, J. M. (2022). 250-Year reconstruction of

460 pollarding events reveals sharp management changes in Iberian ash woodlands. *Trees*,

461 *36*(6), 1909–1921. https://doi.org/10.1007/s00468-022-02343-8

462 Chollet, F. (2015). *Keras*. Keras. https://keras.io/

463 Dobrilovič, M. (2010). Vegetation Elements in Baroque Gardens (The Influence of Foreign

464 Plants on The Baroque Programme). *Acta Horticulturae*, *881*, 899–904.

465 https://doi.org/10.17660/ActaHortic.2010.881.151

466 Du, S., Lindenbergh, R., Ledoux, H., Stoter, J., & Nan, L. (2019). AdTree: Accurate, Detailed,

467 and Automatic Modelling of Laser-Scanned Trees. *Remote Sensing*, *11*(18), Article 18.

468 https://doi.org/10.3390/rs11182074

469 Fan, G., Nan, L., Dong, Y., Su, X., & Chen, F. (2020). AdQSM: A New Method for

470 Estimating Above-Ground Biomass from TLS Point Clouds. *Remote Sensing*, *12*(18),

471 Article 18. https://doi.org/10.3390/rs12183089

472 Girardeau-Montaut, D. (2023). *Cloud-to-Cloud Distance—CloudCompareWiki* [Open-source

473 document]. Cloud-to-Cloud Distance.

474 https://www.cloudcompare.org/doc/wiki/index.php/Cloud-to-Cloud_Distance

475 Gobeawan, L., Lin, E. S., Tandon, A., Yee, A. T. K., Khoo, V. H. S., Teo, S. N., Yi, S., Lim, C.

476 W., Wong, S. T., & Wise, D. J. (2018). MODELING TREES FOR VIRTUAL

477   SINGAPORE: FROM DATA ACQUISITION TO CITYGML MODELS.

478   *International Archives of the Photogrammetry, Remote Sensing & Spatial Information*

479   *Sciences*.

480 Gomez-Roldan, V., Fermas, S., Brewer, P. B., Puech-Pagès, V., Dun, E. A., Pillot, J.-P.,

481   Letisse, F., Matusova, R., Danoun, S., Portais, J.-C., Bouwmeester, H., Bécard, G.,

482   Beveridge, C. A., Rameau, C., & Rochange, S. F. (2008). Strigolactone inhibition of

483   shoot branching. *Nature*, *455*(7210), Article 7210. https://doi.org/10.1038/nature07271

484 Grechi, I., Persello, S., Boudon, F., & Normand, F. (2022). Pruning intensity and severity

485   affect flowering processes in the mango tree. *Acta Horticulturae*, *1346*, 67–74.

486   https://doi.org/10.17660/ActaHortic.2022.1346.9

487 Hackenberg, J., Morhart, C., Sheppard, J., Spiecker, H., & Disney, M. (2014). Highly

488   Accurate Tree Models Derived from Terrestrial Laser Scan Data: A Method

489   Description. *Forests*, *5*(5), Article 5. https://doi.org/10.3390/f5051069

490 Hauer, R., Dawson, J., & Werner, L. (2006). Trees and Ice Storms: The Development of Ice

491   Storm–Resistant Urban Tree Populations (Second Edition). *USDA Forest Service /*

492   *UNL Faculty Publications*. https://digitalcommons.unl.edu/usdafsfacpub/295

493 Hill, J. L., & Hollender, C. A. (2019). Branching out: New insights into the genetic regulation

494   of shoot architecture in trees. *Current Opinion in Plant Biology*, *47*, 73–80.

495   https://doi.org/10.1016/j.pbi.2018.09.010

496 Hirt, P.-R., Xu, Y., Hoegner, L., & Stilla, U. (2021). Change Detection of Urban Trees in MLS

497   Point Clouds Using Occupancy Grids. *PFG – Journal of Photogrammetry, Remote*

498   *Sensing and Geoinformation Science*, *89*(4), 301–318. https://doi.org/10.1007/s41064-

499   021-00179-4

500 Jafari, B., Khaloo, A., & Lattanzi, D. (2017). Deformation Tracking in 3D Point Clouds Via

501   Statistical Sampling of Direct Cloud-to-Cloud Distances. *Journal of Nondestructive*

502   *Evaluation*, *36*(4), 65. https://doi.org/10.1007/s10921-017-0444-2

503   Kohek, Š., Guid, N., Tojnko, S., Unuk, T., & Kolmanič, S. (2015). EduAPPLE: Interactive

504   Teaching Tool for Apple Tree Crown Formation. *HortTechnology*, *25*(2), 238–246.

505   https://doi.org/10.21273/HORTTECH.25.2.238

506   Kotsiantis, S. (2007). Supervised Machine Learning: A Review of Classification Techniques.

507   *Informatica (Slovenia)*, *31*, 249–268.

508   Kükenbrink, D., Marty, M., Bösch, R., & Ginzler, C. (2022). Benchmarking laser scanning

509   and terrestrial photogrammetry to extract forest inventory parameters in a complex

510   temperate forest. *International Journal of Applied Earth Observation and*

511   *Geoinformation*, *113*, 102999. https://doi.org/10.1016/j.jag.2022.102999

512   Leica. (2023). *Leica Zeno FLX100 plus | Smartantenne* [Leica Zeno FLX100 plus

513   Smartantenne - Eine genaue, kompakte und flexible Lösung für alle]. https://leica-

514   geosystems.com/de-de/products/gis-collectors/smart-antennas/leica-zeno-flx100-plus

515   Li, J., Wu, H., Xiao, Z., & Lu, H. (2022). 3D modeling of laser-scanned trees based on

516   skeleton refined extraction. *International Journal of Applied Earth Observation and*

517   *Geoinformation*, *112*, 102943. https://doi.org/10.1016/j.jag.2022.102943

518   Li, M., Ma, L., Zong, W., Luo, C., Huang, M., & Song, Y. (2021). Design and Experimental

519   Evaluation of a Form Trimming Machine for Horticultural Plants. *Applied Sciences*,

520   *11*(5), Article 5. https://doi.org/10.3390/app11052230

521   Liu, Y., Guo, J., Benes, B., Deussen, O., Zhang, X., & Huang, H. (2021). TreePartNet: Neural

522   decomposition of point clouds for 3D tree reconstruction. *ACM Transactions on*

523   *Graphics*, *40*(6). https://doi.org/10.1145/3478513.3480486

524   Martín-Fontecha, E. S., Tarancón, C., & Cubas, P. (2018). To grow or not to grow, a power-

525   saving program induced in dormant buds. *Current Opinion in Plant Biology*, *41*, 102–

526   109. https://doi.org/10.1016/j.pbi.2017.10.001

527   Martini, A. M. Z., Lima, R. A. F., Franco, G. A. D. C., & Rodrigues, R. R. (2008). The need

528   for full inventories of tree modes of disturbance to improve forest dynamics

529   comprehension: An example from a semideciduous forest in Brazil. *Forest Ecology*

530   *and Management*, *255*(5), 1479–1488. https://doi.org/10.1016/j.foreco.2007.11.004

531   Matula, R., Šrámek, M., Kvasnica, J., Uherková, B., Slepička, J., Matoušková, M., Kutchartt,

532   E., & Svátek, M. (2019). Pre-disturbance tree size, sprouting vigour and competition

533   drive the survival and growth of resprouting trees. *Forest Ecology and Management*,

534   *446*, 71–79. https://doi.org/10.1016/j.foreco.2019.05.012

535   Pandala, S. R. (2023, July 19). *GitHub Master—Shankarpandala/lazypredict*. GitHub.

536   https://github.com/shankarpandala/lazypredict/blob/master/docs/index.rst

537   Pedregosa, F., Varoquaux, G., Gramfort, A., Michel, V., Thirion, B., Grisel, O., Blondel, M.,

538   Prettenhofer, P., Weiss, R., Dubourg, V., Vanderplas, J., Passos, A., Cournapeau, D.,

539   Brucher, M., Perrot, M., & Duchesnay, É. (2011). Scikit-learn: Machine Learning in

540   Python. *Journal of Machine Learning Research*, *12*(85), 2825–2830.

541   Petit, S., & Watkins, C. (2003). Pollarding Trees: Changing Attitudes to a Traditional Land

542   Management Practice in Britain 1600–1900. *Rural History*, *14*(2), 157–176.

543   https://doi.org/10.1017/S0956793303001018

544   Raumonen, P., Kaasalainen, M., Åkerblom, M., Kaasalainen, S., Kaartinen, H., Vastaranta, M.,

545   Holopainen, M., Disney, M., & Lewis, P. (2013). Fast Automatic Precision Tree

546   Models from Terrestrial Laser Scanner Data. *Remote Sensing*, *5*(2), Article 2.

547   https://doi.org/10.3390/rs5020491

548   RIEGL, L. M. S. G. (2023). *RIEGL - Produktdetail*. RIEGL - Produktdetail.

549   http://www.riegl.com/nc/products/terrestrial-

550   scanning/produktdetail/product/scanner/48/

551   Rusinkiewicz, S., & Levoy, M. (2001). Efficient variants of the ICP algorithm. *Proceedings*

552   *Third International Conference on 3-D Digital Imaging and Modeling*, 145–152.

553   https://doi.org/10.1109/IM.2001.924423

554   Rusu, R. B., & Cousins, S. (2011). 3D is here: Point Cloud Library (PCL). *2011 IEEE*

555   *International Conference on Robotics and Automation*, 1–4.

556   https://doi.org/10.1109/ICRA.2011.5980567

557   Salam, B. B., Barbier, F., Danieli, R., Teper-Bamnolker, P., Ziv, C., Spíchal, L., Aruchamy, K.,

558   Shnaider, Y., Leibman, D., Shaya, F., Carmeli-Weissberg, M., Gal-On, A., Jiang, J.,

559   Ori, N., Beveridge, C., & Eshel, D. (2021). Sucrose promotes stem branching through

560   cytokinin. *Plant Physiology*, *185*(4), 1708–1721.

561   https://doi.org/10.1093/plphys/kiab003

562   Salama, K. (2021). *Keras documentation: Node Classification with Graph Neural Networks*.

563   https://keras.io/examples/graph/gnn_citations/

564   Sam, S., Mira, L., & Kai, S. (2022). The impact of digitalization and automation on

565   horticultural employees – A systematic literature review and field study. *Journal of*

566   *Rural Studies*, *95*, 560–569. https://doi.org/10.1016/j.jrurstud.2022.09.016

567   Samuel, A. L. (1959). Some Studies in Machine Learning Using the Game of Checkers. *IBM*

568   *Journal of Research and Development*, *3*(3), 210–229.

569   https://doi.org/10.1147/rd.33.0210

570   Saunders, W. (1898). *Pruning of Trees and Other Plants*. US Department of Agriculture.

571   https://naldc.nal.usda.gov/download/IND43620311/PDF

572   Saure, M. C. (1987). Summer pruning effects in apple—A review. *Scientia Horticulturae*,

573   *30*(4), 253–282. https://doi.org/10.1016/0304-4238(87)90001-X

574   Schneider, A., Boudon, F., Demotes-Mainard, S., Sakr, S., Godin, C., & Bertheloot, J. (2022).

575   *Control of lateral meristems: How is sugar availability involved in the environmental*

576   *control of axillary bud outgrowth?* [Conference_item]. From Genes to Plant

577   Architecture: The Shoot Apical Meristem in All Its States; INRAE.

578   https://agritrop.cirad.fr/603143/

579   Shu, Q., Rötzer, T., Detter, A., & Ludwig, F. (2022). Tree Information Modeling: A Data

580   Exchange Platform for Tree Design and Management. *Forests*, *13*(11), Article 11.

581   https://doi.org/10.3390/f13111955

582   Simler, A. B., Metz, M. R., Frangioso, K. M., Meentemeyer, R. K., & Rizzo, D. M. (2018).

583   Novel disturbance interactions between fire and an emerging disease impact survival

584   and growth of resprouting trees. *Ecology*, *99*(10), 2217–2229.

585   https://doi.org/10.1002/ecy.2493

586   Singh, R. K., Bhalerao, R. P., & Maurya, J. P. (2022). When to branch: Seasonal control of

587   shoot architecture in trees. *The FEBS Journal*, *289*(24), 8062–8070.

588   https://doi.org/10.1111/febs.16227

589   Sun, J., Wang, P., Li, R., Zhou, M., & Wu, Y. (2022). Fast Tree Skeleton Extraction Using

590   Voxel Thinning Based on Tree Point Cloud. *Remote Sensing*, *14*(11), Article 11.

591   https://doi.org/10.3390/rs14112558

592   Suzuki, A. (2002). Influence of shoot architectural position on shoot growth and branching

593   patterns in Cleyera japonica. *Tree Physiology*, *22*(12), 885–889.

594   https://doi.org/10.1093/treephys/22.12.885

595   The MathWorks Inc. (2023). *MATLAB version: 9.13.0 (R2022b)* [Computer software]. The

596   MathWorks Inc. https://www.mathworks.com

597   Tosto, A., Evers, J. B., Anten, N. P. R., & Zuidema, P. A. (2023). *Branching responses to*

598   *pruning in cocoa* [Preprint]. Plant Biology. https://doi.org/10.1101/2023.03.08.531700

599   Wang, Z., Zhang, L., Fang, T., Mathiopoulos, P. T., Qu, H., Chen, D., & Wang, Y. (2014). A

600   Structure-Aware Global Optimization Method for Reconstructing 3-D Tree Models

601   From Terrestrial Laser Scanning Data. *IEEE Transactions on Geoscience and Remote*

602   *Sensing*, *52*(9), 5653–5669. https://doi.org/10.1109/TGRS.2013.2291815

603   Yang, J., Wen, X., Wang, Q., Ye, J.-S., Zhang, Y., & Sun, Y. (2022). A Novel Algorithm Based

604   on Geometric Characteristics for Tree Branch Skeleton Extraction from LiDAR Point

605   Cloud. *Forests*, *13*(10), Article 10. https://doi.org/10.3390/f13101534

606   Yazdi, H., Shu, Q., & Ludwig, F. (2023). A Target-driven Tree Planting and Maintenance

607   Approach for Next Generation Urban Green Infrastructure (UGI). *JoDLA – Journal of*

608   *Digital Landscape Architecture*, *8–2023*, 178. https://doi.org/10.14627/537740019

609

610   Supplementary Materials
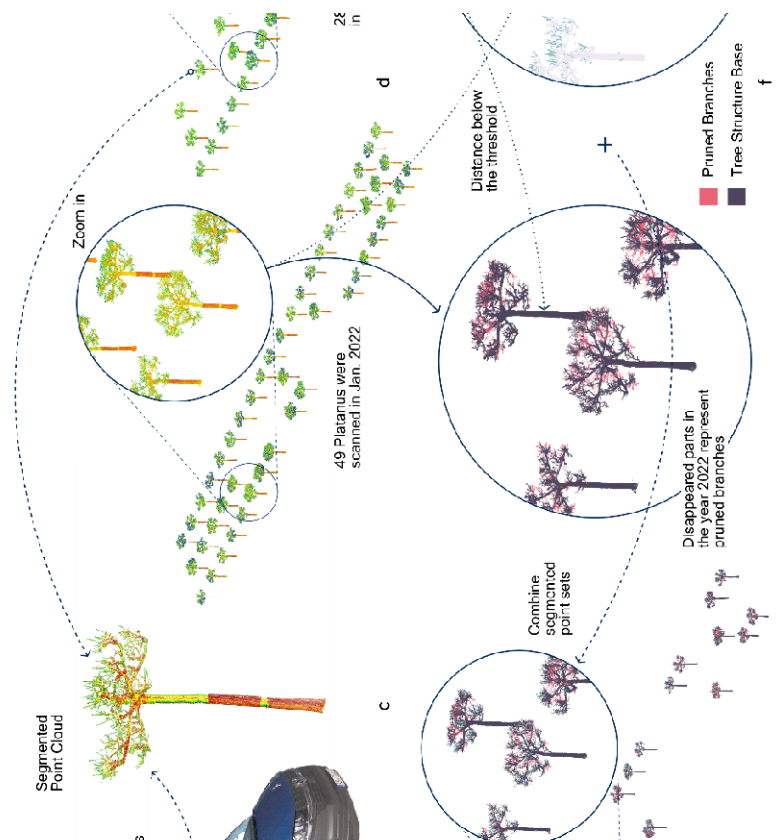
611

612   Appendix 1. An overview of the workflow for point cloud acquiring and pre-processing

613

614   Appendix 2. Correlations between each two attributes of the dataset. The number of new

615   shoots is indicated with the colour, a darker colour represents a larger number of new shoots

616   on the cylinder. The value "-1" is marked as pruned out cylinders.

617

618

619   Appendix 3. Visualizing the evaluation of the LGBMClassifier and GaussianNB models in

620   predicting resprouting patterns. The ground truths are illustrated in the middle. The binary

621   predictions using LGBMClassifier are drawn on the lower left side while the multiclass

622   predictions using GaussianNB model are drawn on the upper right.

keep only 6 soft branches at ca. 3 meter height

bend the 6 branches towards different directions with supporting bamboos

New Shoots   Tree Structure Base   Pruned Branches

1st year - Early Spring
Pruning, Bending and Fixation

2nd-6th year - August
Detailed Pruning

6th year
Ready for Deliver

Table-topped Platanus ×hispanica

a

LiDAR Scans

b

Segmented Point Cloud

c

Zoom in

49 Platanus were scanned in Jan. 2022
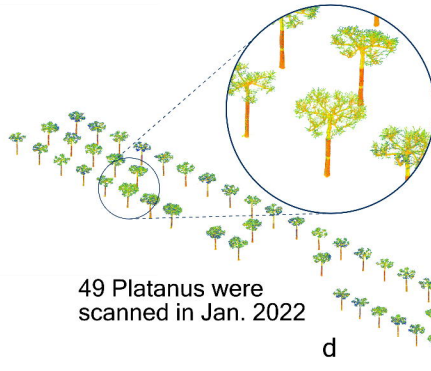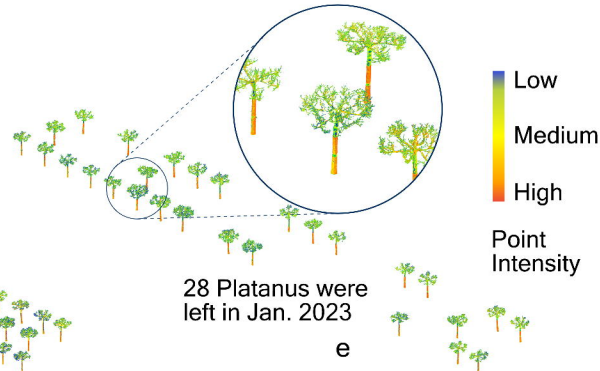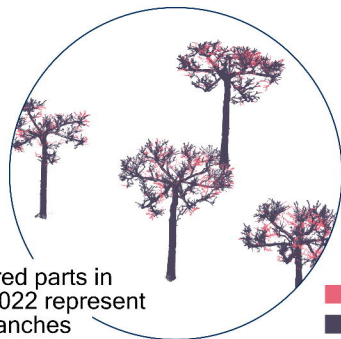
d

Zoom in

28 Platanus were left in Jan. 2023

e

Point Intensity

Low
Medium
High

Disappeared parts in the year 2022 represent pruned branches

Pruned Branches
Tree Structure Base

f

+

Appeared parts in the year 2023 represent new shoots

New Shoots
Leave Out Structure

g

=

Pruned Branches
New Shoots
Tree Structure Base

h

Point Cloud Scanned in 2022

TreeQSM reconstruction

QSM Model of the Tree in 2022

Branch Order 4
Branch Order 3
Branch Order 2
Branch Order 1
Branch Order 0

Pruned Branches
New Shoots
Tree Structure Base

Low
Medium
High

Point Intensity

Point Cloud Scanned in 2023

TreeQSM reconstruction

QSM Model of the Tree in 2023

Segmented Point Cloud from Pre-processing

Labeling in reference to the segmented point cloud

a

b

c

Count the number of new shoots on the structure base

3 New Children
2 New Children
1 New Children
0 New Children

Pruned Branches
New Shoots
Tree Structure Base

Labelled QSM Model of the Tree in 2022

Merge the corresponding QSMs into one

3 Pruned Children
2 Pruned Children
1 Pruned Children
0 Pruned Children

Count the number of pruned branches on the structure base

Structure Base

Merged QSM

Labelled QSM Model of the Tree in 2023

d

e

f

ReLU

ReLU

treeID
branchID
branchOrder
cylinderID
posInBranch
parentCyID
childCyID
start_x
start_y
start_z
axis_x
axis_y
axis_z
length
radius
isAddedVirtual
isCutCylinder

Sigmoid

× 64

× 128

Input Layer

Hidden Layers

Output Layer

Node (new shoot number = 0)
Node (new shoot number = 1)
Node (new shoot number = 2)
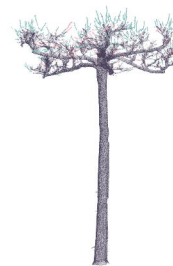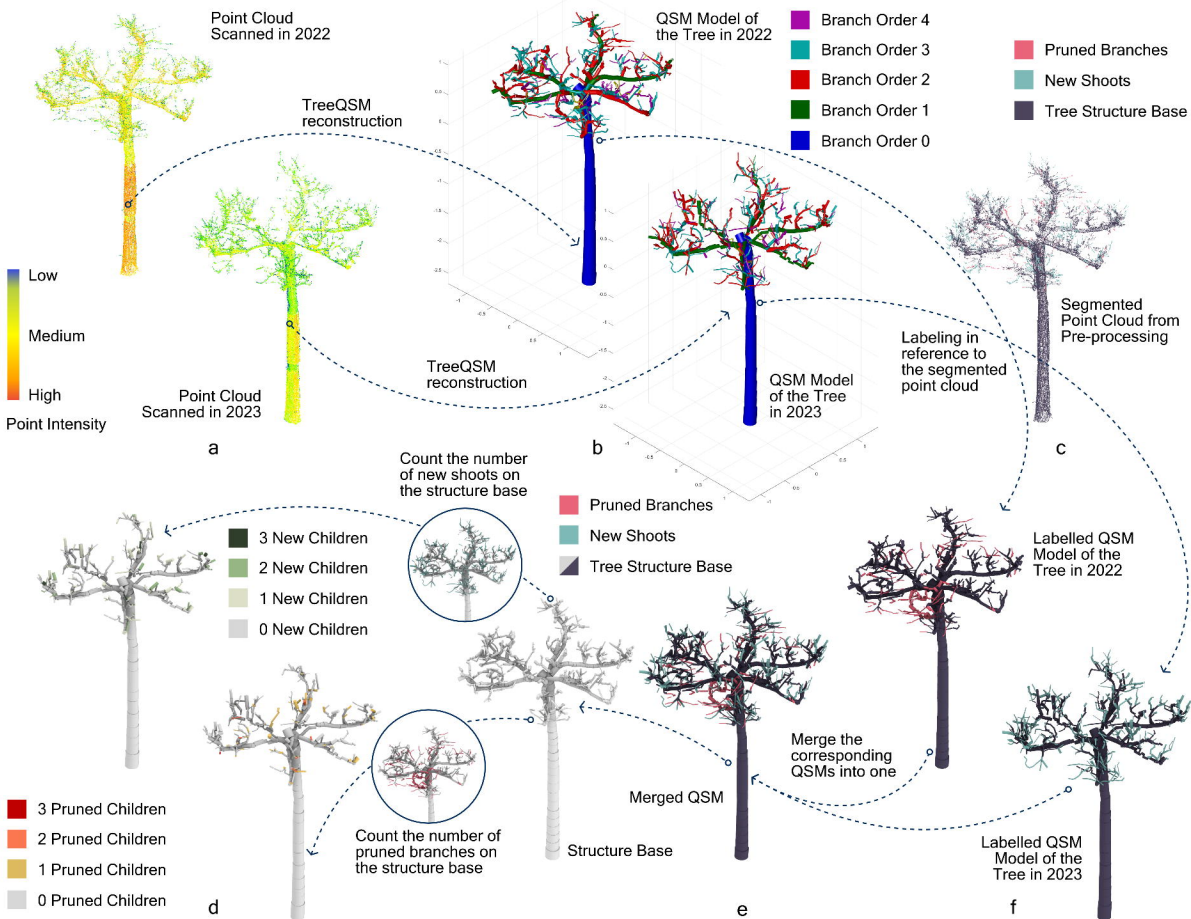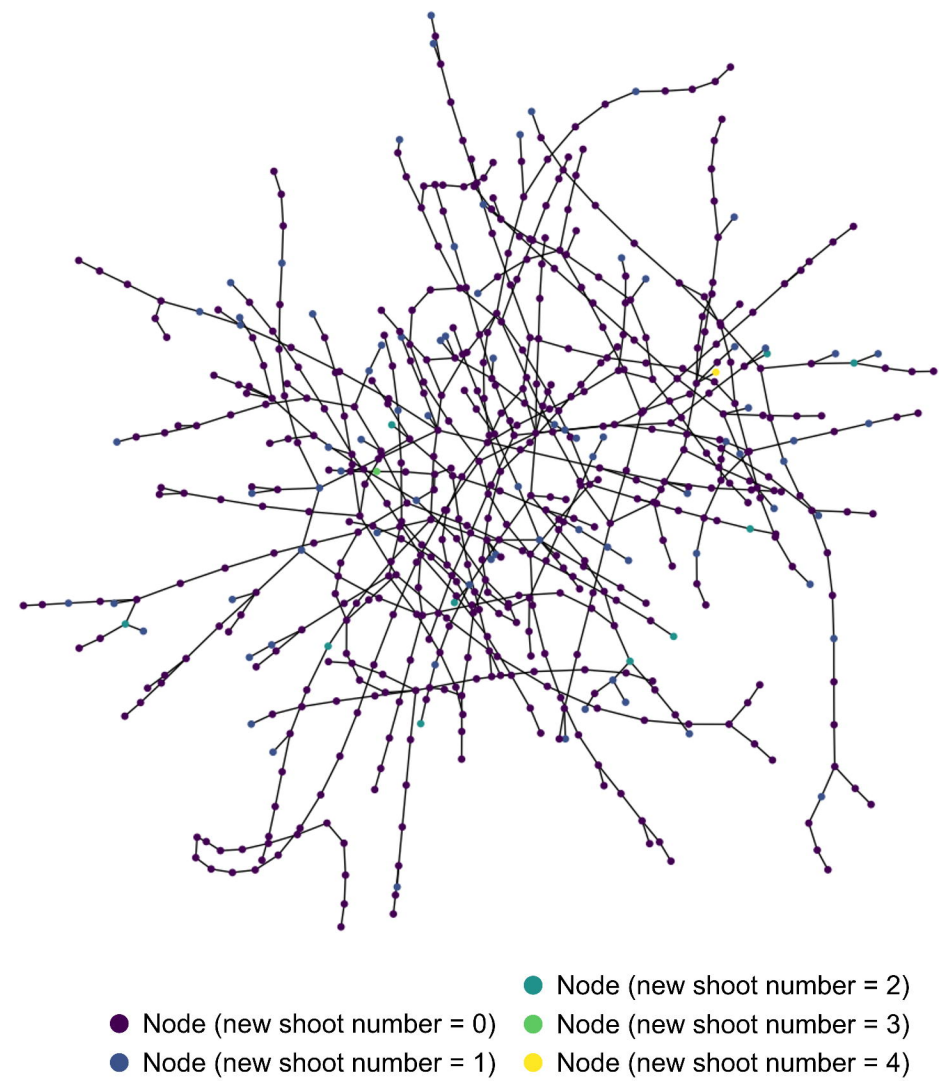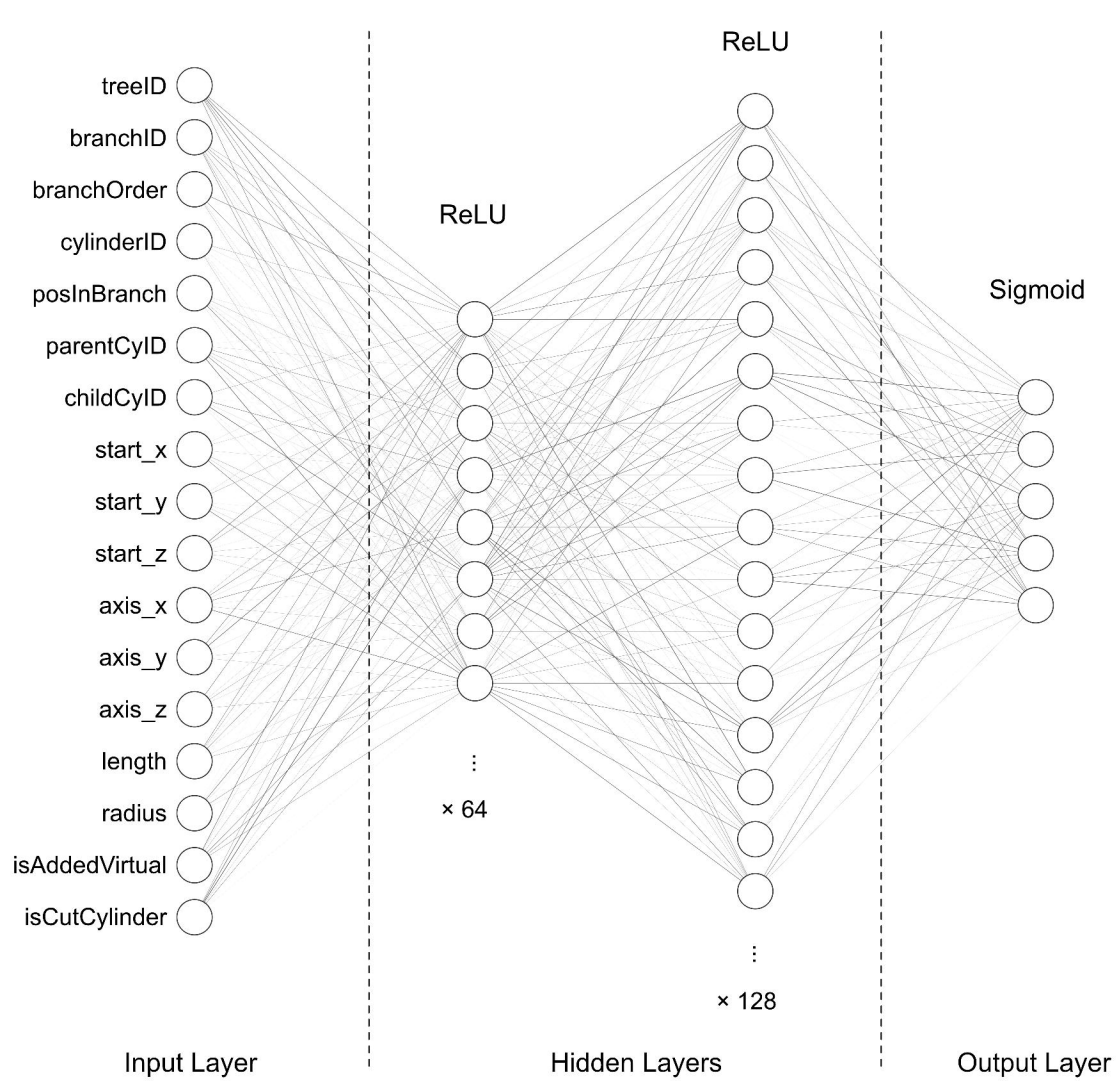Node (new shoot number = 3)
Node (new shoot number = 4)

Benchmark of Classification Models for Both Binary and Multiclass Labels